Helical Structures

DOI: 10.1002/ange.200503136

Two-Dimensional Hierarchical Self-Assembly of One-Handed Helical Polymers on Graphite

Shin-ichiro Sakurai, Kento Okoshi, Jiro Kumaki, and Eiji Yashima**

The control and fabrication of ordered 2D arrays of molecules, in particular chiral (macro)molecules on substrates, is among the great challenges in materials science as these systems have attractive applications in chemical sensing, electro-optical devices, enantioselective adsorbents, and catalysis.[1] The concept of supramolecular self-assembly has been widely applied to the epitaxial alignments of chiral molecules on crystalline graphite and metals to create chiral surfaces, and their enantiomorphic 2D arrangements have been visualized by scanning probe microscopy (SPM).[2] However, it is still difficult to exploit biological and synthetic helical polymers[3] for the creation of 2D chiral surfaces by self-assembly because of their unfavorable strong surface interactions, which can compete with intermolecular interactions and change their inherent helical conformations, except for preorganized DNA with specific sequences[4] and nanopatterned collagen formed by dip-pen nanolithography.[5] Herein we show that cholesteric liquid-crystalline helical polyacetylenes self-assemble into ordered, 2D layered crystals on highly oriented pyrolytic graphite (HOPG). Flat monolayers epitaxially form on the basal plane of the HOPG, on which rodlike helical polyacetylenes further self-assemble into 2D helix-bundles with controlled molecular packing, helical pitch, and handedness upon exposure to organic solvents. The helical conformations in 2D crystals are visualized by atomic force microscopy (AFM) with molecular resolution and the results quantified by X-ray diffraction of the oriented liquid-crystalline polymer films.

Stereoregular (*cis–transoid*) poly(phenylacetylene) bearing L- or D-alanine residues with a long alkyl chain as pendants (namely, poly-**1L** and poly-**1D**, respectively; Figure 1a) were prepared according to a previously reported method.[6] The circular dichroism (CD) spectra of poly-**1L** and poly-**1D** in dilute benzene solution showed characteristic Cotton effects in the polymer backbone region (250–450 nm) that are mirror images of each other (Figure 1b), which indicates that the polymers have a predominantly one-handed

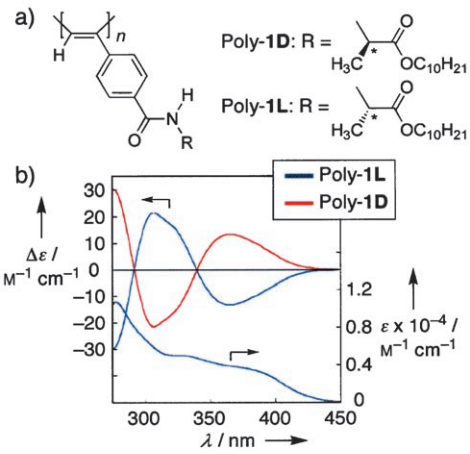

Figure 1. Chiroptical properties of poly-**1** in benzene. a) Structures of poly-**1D** and poly-**1L**. b) CD spectra of poly-**1L** and poly-**1D** in benzene. The absorption spectrum of poly-**1L** in benzene is also shown.

helical conformation with exactly the same helical structure except for the sense of their helicity.[6] Among a variety of helical polyacetylenes prepared so far, the polymers have an exceptionally rigid-rod main-chain character; this has allowed the formation of the first polyacetylene-based cholesteric liquid crystals in concentrated solutions.[6] The interplay between the chirality of the pendant groups, the macromolecular helicity, and the chirality at a macroscopic level is of great interest from fundamental and biological viewpoints. To this end, we have investigated the structures of the helical polymers on HOPG with AFM.

Figure 2a shows a typical AFM image of poly-**1L** spin cast on HOPG from a dilute benzene solution. The poly-**1L** molecules spontaneously self-assembled into a highly ordered monolayer as evidenced by parallel stripes with a periodicity of 4.72 ± 0.21 nm. On this 2D ordered first monolayer, irregular amorphous-like polymers with a height of 0.94 ± 0.3 nm were deposited (second layer as indicated by a red arrow in Figure 2a). The 2D fast Fourier transforms of this first layer showed threefold symmetry, which reflects the crystallographic structure of the HOPG substrate. The average corrugation height of the surface was 0.12 ± 0.02 nm from the profiles of the cross sections included in Figure 2a. The average height of the first monolayer was 0.38 ± 0.04 nm as derived from AFM observations of the isolated poly-**1L** monolayers prepared from a dilute solution in benzene ($0.01\ mg\,mL^{-1}$; see Supporting Information), which was less than the molecular diameter of a helical poly-**1** model (2.1 nm). These results indicate that the poly-**1L** molecules lie flat on the substrate with a planar conformation aligned parallel to the graphite lattice, probably because of the strong and epitaxial adsorption of the long pendant alkyl chains on HOPG; the chain-to-chain spacing of the first layer observed by AFM agreed with that of a model for aligned planar poly-**1** chains (Figure 2d, left). Similar epitaxial alignments on HOPG of long alkyl compounds and some macromolecules with long pendant alkyl chains were reported.[7]

Although the second layer of polymers deposited on the first layer appeared to be amorphous with no specific

[*] Dr. S.-i. Sakurai, Dr. K. Okoshi, Dr. J. Kumaki, Prof. E. Yashima
Yashima Super-Structured Helix Project
Exploratory Research for Advanced Technology (ERATO)
Japan Science and Technology Agency (JST)
101 Creation Core Nagoya, Shimoshidami, Moriyama-ku
Nagoya 463–0003 (Japan)
Fax: (+81) 52-739-2083
E-mail: kumaki@yp-jst.jp
yashima@apchem.nagoya-u.ac.jp

Supporting information for this article is available on the WWW under http://www.angewandte.org or from the author.

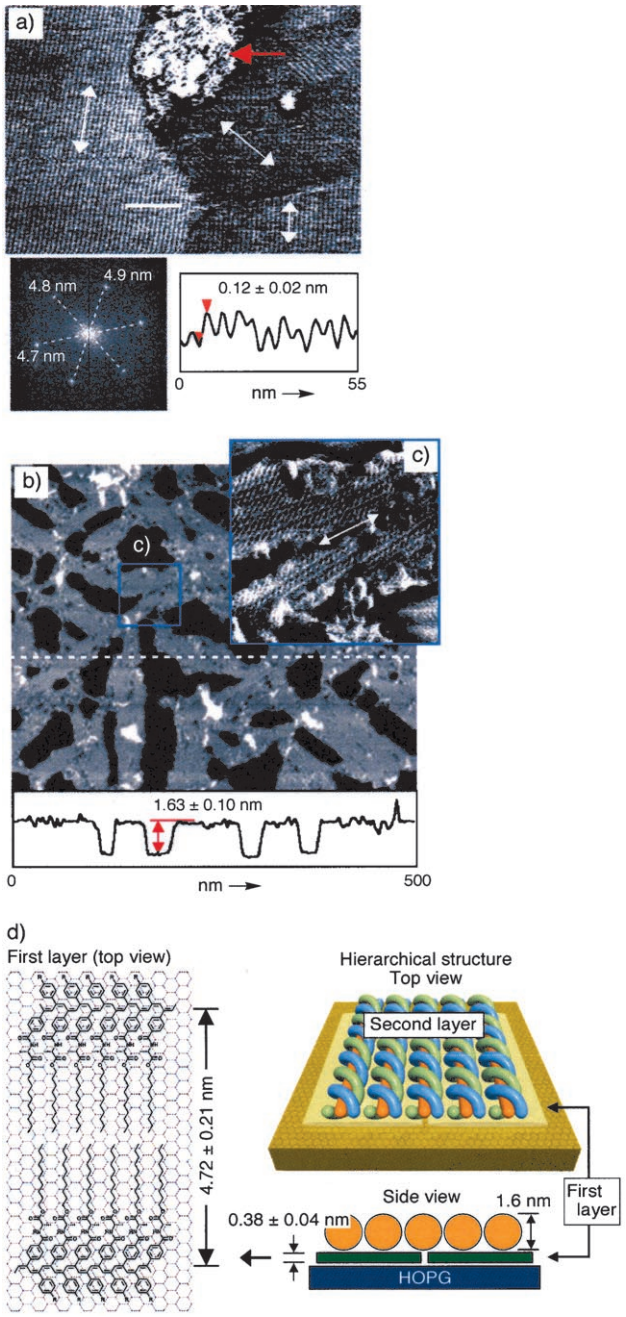

Figure 2. AFM observation of molecular ordering of poly-**1** on HOPG. a) AFM phase image of the epitaxial poly-**1L** crystals prepared by spin casting a dilute solution in benzene (0.05 mg mL^{-1}) on HOPG. The white arrows in the AFM image indicate the direction of the main-chain axes of the polymer; the red arrow indicates the amorphous polymer chains (scale: 250×350 nm). The cross-sectional profile shown by a white line and the typical 2D fast Fourier transform are also shown. b) AFM height image of poly-**1L** prepared by spin casting a solution in benzene (0.1 mg mL^{-1}) on HOPG followed by exposure to benzene vapor for 12 h at ambient temperature (ca. 22 °C; scale: 400×500 nm). The cross-sectional profile denoted by the white dashed line is also shown. c) High-magnification AFM phase image of poly-**1L** corresponding to the area indicated by the blue square in (b). The white arrow in the image indicates the direction of the main-chain axes of the polymer (scale: 70×70 nm). The 2D self-assembled poly-**1L** chains with a left-handed twisted structure can be clearly seen. d) Schematic representation of the hierarchical structure of the self-assembled poly-**1L** on HOPG.

structures, when exposed to benzene vapor for 12 h they further self-assembled into well-defined helix bundles with a constant height of 1.63 ± 0.10 nm (Figure 2b; see Supporting Information for its phase image). The orientation of the polymer strands in the second layer, which was anticipated to be influenced by that of the first layer, was nearly parallel to the polymer backbones underneath (first layer) and had approximately threefold symmetry (see Supporting Information). In the high-resolution AFM image (Figure 2c), the bundle structures are clearly resolved into individual left-handed helical poly-**1L** chains packed parallel to each other. Consequently, the first layer of the poly-**1** lamellae epitaxially deposited on the HOPG basal plane could not only prevent unfavorable direct interactions between helical poly-**1** chains and the HOPG but also serve as a template or soft nanoscopic "rails"[8] for subsequent formation of the upper-layer helix bundle with controlled helicity and lateral packing (Figure 2d, right).

Figure 3a and b show high-resolution AFM phase images of typical 2D arrangements of poly-**1L** and poly-**1D** (second layer) together with their magnified images after exposure to benzene vapor (Figure 3d).[9] These AFM images illustrate possible helical pitch and chain arrangements. As shown in Figure 3d, the 2D molecular ordering of each polymer consists of one-handed helical polymer chains in parallel arrangement; chain–chain spacing (2.13 ± 0.11 nm for poly-**1L** and 2.18 ± 0.10 nm for poly-**1D**) and helical pitch (2.34 ± 0.21 nm for poly-**1L** and 2.47 ± 0.18 nm for poly-**1D**) are similar for poly-**1L** and poly-**1D**.[10] The periodic oblique stripes (blue and green lines in Figure 3d AFM images), which originate from a one-handed helical array of the pendants, were tilted anticlockwise or clockwise at −41 and +42°, respectively, with respect to the axis of the main chain (red arrows in Figure 3a, b, and d). The tilt angles are constant irrespective of the direction of the chains. Some additional AFM images for different areas are shown in the Supporting Information. This remarkable 2D mirror-image relationship suggests that upon exposure to benzene vapor, poly-**1L** and poly-**1D** have enantiomeric left- and right-handed helical structures, respectively, with respect to the pendant arrangements.[11]

The 3D solid-state structure of poly-**1L** was investigated by X-ray analysis. Figure 3c shows a wide-angle X-ray diffraction (WAXD) pattern of a poly-**1L** film prepared from a concentrated cholesteric liquid-crystalline benzene solution and oriented in one direction. The WAXD pattern of the film shows diffuse-but-apparent meridional reflections on the lines of the 5th and 11th layers that are assignable to the turn-layer line and the unit height, respectively, thus giving a helix with 11 units per 5 turns and a translational length per unit of 0.212 nm (for more details, see the Supporting Information). Thus, the helical pitch estimated by AFM is in good agreement with the half pitch of the helical arrangements of the pendants as determined by X-ray analysis (2.33 nm), whereas the chain–chain spacing was slightly larger than that deduced from the WAXD pattern (1.97 nm) because the lateral spacing may be affected by hydrophobic interactions of epitaxially adsorbed pendant alkyl chains of

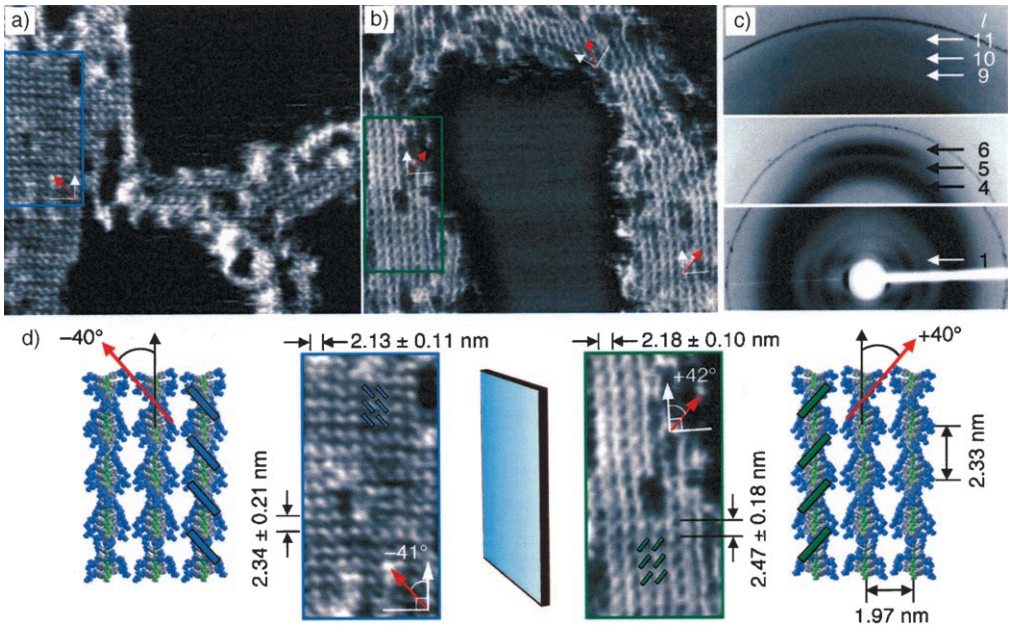

Figure 3. AFM images of self-assembled poly-**1** on HOPG and helical structures of poly-**1** proposed by X-ray analysis. AFM phase images of self-assembled a) poly-**1L** and b) poly-**1D**. The samples were prepared by spin casting solutions in benzene (0.1 mg mL^{-1}) on HOPG, followed by exposure to benzene vapor for 12 h at ambient temperature (ca. 20 °C; scale: 80×90 nm). c) WAXD patterns of an oriented poly-**1L** film prepared from a concentrated cholesteric liquid-crystal benzene solution (ca. 20 wt %). d) Magnified AFM phase images of poly-**1L** (middle left) and poly-**1D** (middle right), which correspond to the area indicated by the squares in (a) and (b), respectively (scale: 20×40 nm). Schematic drawings of the mirror-image relationship of helical poly-**1L** (middle left) and poly-**1D** (middle right; blue and green lines, respectively) 2D crystals with antipodal oblique pendant arrangements are also shown. Possible models (left and right) were constructed on the basis of the results of X-ray structural analysis.

the first layer of the poly-**1** lamellae (for comparison between the AFM and X-ray results, see the Supporting Information).

These AFM observations combined with X-ray structural analysis suggest that the helices of the poly-**1L** and poly-**1D** single chains are enantiomers, and both the enantiomeric left- and right-handed helical poly-**1** polymers provide the enantiomorphic 2D structures on the surface. In spite of extensive studies, determination of the absolute sense of helicity of biological and synthetic polymers still remains a difficult problem. Previous efforts have attempted to observe single macromolecules on surfaces by SPM.[12] Our approach based on the supramolecular self-assembly into a well-defined 2D crystal formation may be superior to previous approaches because the helical conformations are maintained in the 2D lattice, which can be easily recognized at high magnification.

In conclusion, we have demonstrated that upon exposure to solvent vapors rigid-rod helical polymers self-assemble to form ordered 2D crystals with a controlled helical conformation on a solid surface. The structures were visualized by AFM with molecular resolution. This system is conceptually new and provides an approach not only for the construction of chiral materials as chiral selectors and catalysts but also for the rational design of switchable chiral surfaces based on inversion of helicity of macromolecules.[3]

Experimental Section

Polymerization: Poly-**1L** and poly-**1D** were prepared according to a previously reported method by using a rhodium catalyst in THF.[6] The number-average molecular weight ($\bar{M}_n$) and the molecular-weight distribution ($\bar{M}_w/\bar{M}_n$; $\bar{M}_w$ is the weight-average molecular weight) for poly-**1L** was $\bar{M}_n = 2.0\times10^5$ and $\bar{M}_w/\bar{M}_n = 2.3$ and for poly-**1D** $\bar{M}_n = 3.2\times10^5$ and $\bar{M}_w/\bar{M}_n = 2.0$ as determined by size-exclusion chromatography with polystyrene standards and $CHCl_3$ as the eluent. All polymers had a highly *cis–transoidal* structure as deduced from their ^{1}H NMR spectra.[6]

Absorption and CD measurements: The absorption spectra were obtained by using a 0.2-mm quartz cell at 6 °C with a Jasco V570 spectrophotometer and CD spectra were obtained with a Jasco J820 spectropolarimeter. The temperature was controlled with a Jasco CDF-426 L instrument. The polymer concentration was calculated on the basis of the monomer unit and was 1.5 mg mL^{-1}.

AFM measurements: Stock solutions of poly-**1L** and poly-**1D** in dry benzene (0.05 and 0.1 mg mL^{-1}) were prepared. Samples for AFM measurements of poly-**1L** and poly-**1D** were prepared by spin casting 10-μL aliquots of the stock solutions of the polymers. The spin casting was carried out at room temperature at 1800 rpm on freshly cleaved HOPG. After the polymers had been deposited on the HOPG, the HOPG substrates were exposed to benzene vapors, then the substrates were dried under vacuum for 2 h. The organic vapors were prepared by putting benzene (1 mL) into a 2-mL flask that was inside a 50-mL flask, and the HOPG substrates were then placed in the 50-mL flask. The AFM measurements were performed by using a Nanoscope IIIa or Nanoscope IV microscope (Veeco Instruments, Santa Barbara, CA) in air at ambient temperature with standard silicon cantilevers (NCH, NanoWorld, Neuchâtel, Switzerland) and super-sharp cantilevers (SSS-NCH) in the tapping mode. Typical settings of the AFM for the high-magnification observations were as follows: amplitude 1.0–1.5 V; set point 0.9–1.4 V; scan rate 2 Hz. The Nanoscope image processing program was used for the image analysis (see also the Supporting Information).

WAXD analysis: Oriented helical poly-**1L** films for X-ray analyses were prepared by shearing one-directionally lyotropic

liquid-crystalline solutions of poly-**1L** in benzene cast on a glass plate. After being dried in air, the oriented poly-**1L** films were floated off the glass substrates onto water, carefully collected, then dried. Several oriented poly-**1L** films were prepared and piled up with the orientation direction parallel for X-ray measurement. X-ray measurements were carried out on a Rigaku RINT RAPID-R X-ray diffractometer with a rotating-anode generator with graphite monochromated $Cu_{K\alpha}$ radiation (0.15418 nm) focused through a 0.3-mm pinhole collimator, which was supplied at 50 kV and 100-mA current, equipped with a curved imaging plate of specimen-to-plate distance 127.4 mm. X-ray photographs were taken at ambient temperature (20–25 °C) from the edge-view position with a beam parallel to the film surface (see also the Supporting Information).

Molecular modeling and calculations: Molecular modeling and molecular-mechanics calculations were conducted with the Compass force field as implemented in the MS Modeling program (version 3.1, Accelrys Inc., San Diego, CA) operated by a PC running under Windows XP (see also the Supporting Information).

Received: September 5, 2005
Revised: November 7, 2005
Published online: January 13, 2006

Keywords: chirality · helical structures · scanning probe microscopy · self-assembly

[1] a) S. De Feyter, F. C. De Schryver, *Chem. Soc. Rev.* **2003**, *32*, 139 – 150; b) S. M. Barlow, R. Raval, *Surf. Sci. Rep.* **2003**, *50*, 201 – 341.

[2] a) L. C. Giancarlo, G. W. Flynn, *Acc. Chem. Res.* **2000**, *33*, 491 – 501; b) S. De Feyter, A. Gesquière, M. M. Abdel-Mottaleb, P. C. M. Grim, F. C. De Schryver, C. Meiners, M. Sieffert, S. Valiyaveettil, K. Müllen, *Acc. Chem. Res.* **2000**, *33*, 520 – 531; c) M. Ortega Lorenzo, C. J. Baddeley, C. Muryn, R. Raval, *Nature* **2000**, *404*, 376 – 379; d) A. Kühnle, T. R. Linderoth, B. Hammer, F. Besenbacher, *Nature* **2002**, *415*, 891 – 893.

[3] For reviews on artificial helical polymers, see a) J.-M. Lehn, *Supramolecular Chemistry*, VCH, Weinheim, **1995**; b) M. M. Green, J.-W. Park, T. Sato, A. Teramoto, S. Lifson, R. L. B. Selinger, J. V. Selinger, *Angew. Chem.* **1999**, *111*, 3329 – 3345; *Angew. Chem. Int. Ed.* **1999**, *38*, 3138 – 3154; c) D. J. Hill, M. J. Mio, R. B. Prince, T. S. Hughes, J. S. Moore, *Chem. Rev.* **2001**, *101*, 3893 – 4011; d) T. Nakano, Y. Okamoto, *Chem. Rev.* **2001**, *101*, 4013 – 4038; e) J. J. L. M. Cornelissen, A. E. Rowan, R. J. M. Nolte, N. A. J. M. Sommerdijk, *Chem. Rev.* **2001**, *101*, 4039 – 4070; f) L. Brunsveld, B. J. B. Folmer, E. W. Meijer, R. P. Sijbesma, *Chem. Rev.* **2001**, *101*, 4071 – 4097; g) M. Fujiki, *Macromol. Rapid Commun.* **2001**, *22*, 539 – 563; h) E. Yashima, K. Maeda, T. Nishimura, *Chem. Eur. J.* **2004**, *10*, 42 – 51.

[4] E. Winfree, F. Liu, L. A. Wenzler, N. C. Seeman, *Nature* **1998**, *394*, 539 – 544.

[5] D. L. Wilson, R. Martin, S. Hong, M. Cronin-Golomb, C. A. Mirkin, D. L. Kaplan, *Proc. Natl. Acad. Sci. USA* **2001**, *98*, 13660 – 13664.

[6] K. Okoshi, K. Sakajiri, J. Kumaki, E. Yashima, *Macromolecules* **2005**, *38*, 4061 – 4064.

[7] a) J. P. Rabe, S. Buchholz, *Science* **1991**, *253*, 424 – 427; b) S. A. Prokhorova, S. S. Sheiko, M. Möller, C.-H. Ahn, V. Percec, *Macromol. Rapid Commun.* **1998**, *19*, 359 – 366; c) E. Mena-Osteritz, A. Meyer, B. M. W. Langeveld-Voss, R. A. J. Janssen, E. W. Meijer, P. Bäuerle, *Angew. Chem.* **2000**, *112*, 2791 – 2796; *Angew. Chem. Int. Ed.* **2000**, *39*, 2680 – 2684. For reviews of single macromolecule observations by AFM, see: d) A. D. Schlüter, J. P. Rabe, *Angew. Chem.* **2000**, *112*, 860 – 880; *Angew. Chem. Int. Ed.* **2000**, *39*, 864 – 883; e) S. S. Sheiko, M. Möller, *Chem. Rev.* **2001**, *101*, 4099 – 4123. For recent examples, see: f) S. S. Sheiko, S. A. Prokhorova, K. L. Beers, K. Matyjaszewski, I. I. Potemkin, A. R. Khokhlov, M. Möller, *Macromolecules* **2001**, *34*, 8354 – 8360; g) C. Ecker, N. Severin, L. Shu, A. D. Schlüter, J. P. Rabe, *Macromolecules* **2004**, *37*, 2484 – 2489; h) N. Severin, J. P. Rabe, D. G. Kurth, *J. Am. Chem. Soc.* **2004**, *126*, 3696 – 3697; i) J. Pyun, C. Tang, T. Kowalewski, J. M. J. Fréchet, C. J. Hawker, *Macromolecules* **2005**, *38*, 2674 – 2685.

[8] N. Severin, J. Barner, A. A. Kalachev, J. P. Rabe, *Nano Lett.* **2004**, *4*, 577 – 579.

[9] Both the height (see the Supporting Information) and phase (Figure 3) AFM images showed identical structures. The phase images are presented here for clarity.

[10] The helical pitch was estimated on the basis of the averaged distance between each oblique stripe that appeared in the AFM height images of the polymers (see the Supporting Information).

[11] We note that when poly-**1L** has a left-handed helical array of the pendants, the main-chain has an opposite, right-handed helical structure.

[12] a) T. Kanno, H. Tanaka, T. Nakamura, H. Tabata, T. Kawai, *Jpn. J. Appl. Phys.* **1999**, *38*, L606 – L607; b) K. Furukawa, K. Ebata, M. Fujiki, *Adv. Mater.* **2000**, *12*, 1033 – 1036; c) J. J. L. M. Cornelissen, J. J. J. M. Donners, R. de Gelder, W. S. Graswinckel, G. A. Metselaar, A. E. Rowan, N. A. J. M. Sommerdijk, R. J. M. Nolte, *Science* **2001**, *293*, 676 – 680; d) K. Shinohara, S. Yasuda, G. Kato, M. Fujita, H. Shigekawa, *J. Am. Chem. Soc.* **2001**, *123*, 3619 – 3620; e) B. S. Li, K. K. L. Cheuk, D. Yang, J. W. Y. Lam, L. J. Wan, C. Bai, B. Z. Tang, *Macromolecules* **2003**, *36*, 5447 – 5450; f) S. Sakurai, A. Ohira, Y. Suzuki, R. Fujito, T. Nishimura, M. Kunitake, E. Yashima, *J. Polym. Sci. A* **2004**, *42*, 4621 – 4640.

